Electronic Supplementary Material (ESI) for Physical Chemistry Chemical Physics.

Supplementary Information

Effects of Electrospray Mechanisms and Structural Relaxation on Polylactide Ion Conformations in the Gas Phase: Insights from Ion Mobility Spectrometry and Molecular Dynamics Simulations

Quentin Duez[1,2,3], Haidy Metwally[3], Sébastien Hoyas[1,2], Vincent Lemaur[2], Jérôme Cornil[2], Julien De Winter[1], Lars Konermann[3*] and Pascal Gerbaux[1*]

[1]*Organic Synthesis and Mass Spectrometry Laboratory, Center of Innovation and Research in Materials and Polymers (CIRMAP)- UMONS, Place du Parc 23, B-7000 Mons, Belgium*

[2]*Laboratory for Chemistry of Novel Materials, Center of Innovation and Research in Materials and Polymers (CIRMAP)- UMONS, Place du Parc 23, B-7000 Mons, Belgium*

[3]*Department of Chemistry, The University of Western Ontario, London, Ontario, N6A 5B7, Canada*

* Corresponding authors: pascal.gerbaux@umons.ac.be and konerman@uwo.ca

This file contains:

Supporting Figures

Figure S1: Dihedral energy profiles generated at the MP2/cc-pVDZ level, corresponding population distributions and comparison between DREIDING and the reparametrized version of DREIDING (NAPOLION). Additional comments concerning the force field parametrization.

Figure S2: MSMS spectra and corresponding ATDs recorded for selected PLA with increasing collisional energy.

Figure S3: Normalized radial distribution for solutes and solvents in a water/acetonitrile droplet containing PLA20.

Figure S4: MD data for droplets containing PLA20 with r_0 = 5.5 nm.

Figure S5: MD data for droplets containing PLA16 with r_0 = 5.5 nm.

Figure S6: MD snapshots of the evaporation of charged droplets with r_0 = 3 nm containing PLA20.

Figure S7: MD data for droplets containing PLA20 with r_0 = 3 nm.

Figure S8: MD data for droplets containing PLA16 with r_0 = 3 nm.

Figure S9: Histograms of $CCS_{relaxed}$ values for CEM and CRM-generated $[PLA16 + 3Na]^{3+}$, $[PLA20 + 3Na]^{3+}$ and $[PLA20 + 4\ Na]^{4+}$.

Table S1: Statistical analysis of $CCS_{relaxed}$ values.

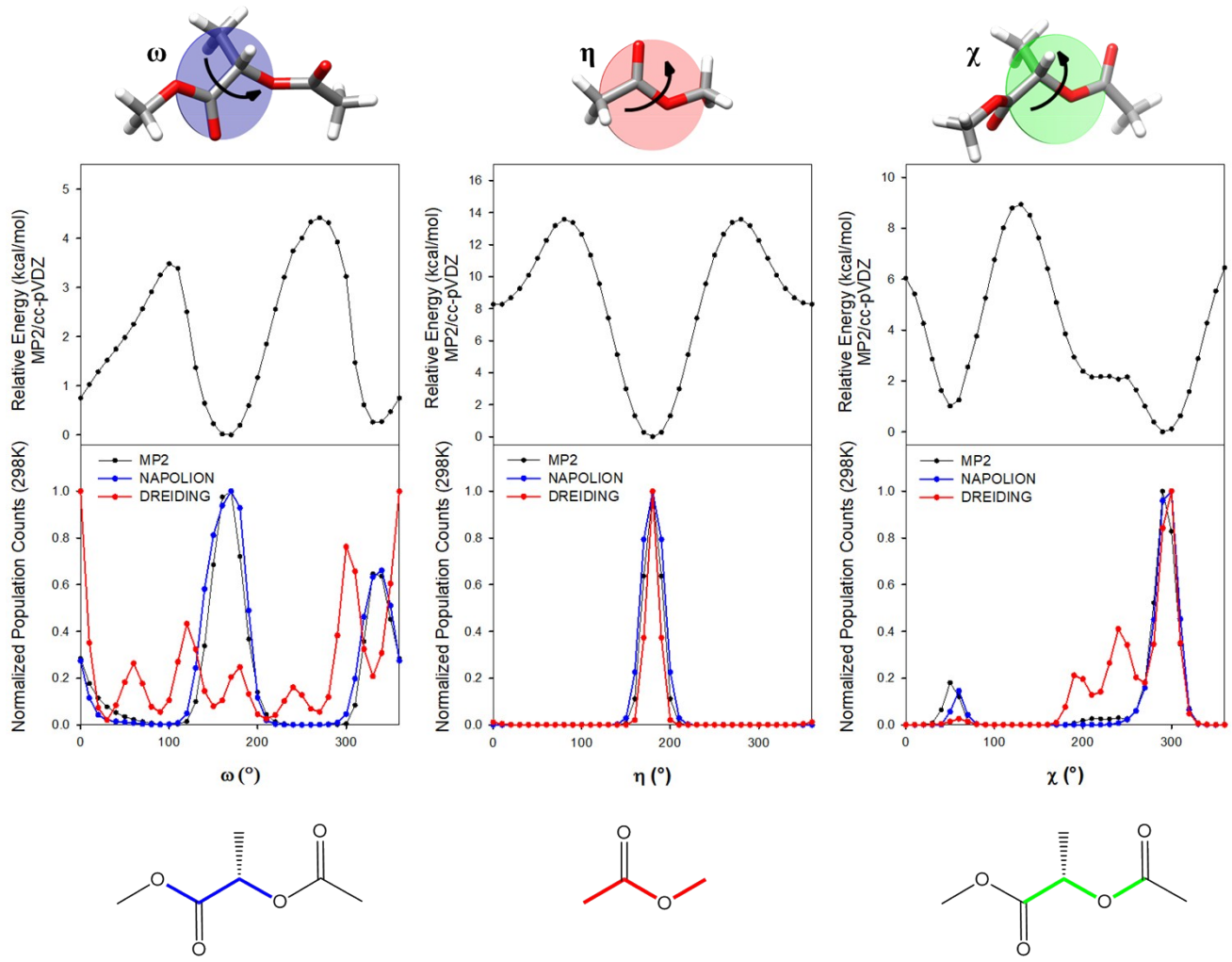

Figure S1. Torsion energy profiles generated at the MP2/cc-pVDZ level (top) for each dihedral angle of interest, denoted **ω**, **η** and **χ**. All geometrical parameters are optimized except for the dihedral of interest when building each torsional profile. These energy profiles are then converted into normalized population distributions (bottom) according to the Boltzmann equation at 298K:

$$\text{Normalized population fraction} = \frac{e^{\frac{-E_I}{kT}}}{\sum_i e^{\frac{-E_I}{kT}}}$$

The same procedure has been carried out at the molecular mechanics level with DREIDING and with our reparametrized force field, NAPOLION. An excellent agreement is found between NAPOLION and quantum-chemical calculations, with a RMSD < 5% obtained for each population profile.

Additional details regarding the parametrization of the Lennard-Jones terms in the force field (See Ref. **Hoyas, S. et al. (2018), PEPDROID: Development of a Generic DREIDING-Based Force Field for the Assessment of Peptoid Secondary Structures. Adv. Theory Simul., 1: 1800089** for more details):

For the reparametrization of equilibrium distance and well depth involving H atoms, Materials Studio 6.0 was used. The electrostatic interactions were described by a purely Coulombic expression (in 1/r) and atomic charges were set according to the COMPASS force field.

Equilibrium distance (R_0) was parametrized through a comparison between experimental collision cross sections (CCS) obtained by Ion Mobility Mass Spectrometry (IMMS) and theoretical values computed on corresponding species. A set of polymer ions with different backbones (PEG, PLA, PCL), chain lengths and charge states was built. Each polymer was submitted to two consecutive quenched MDs at 600 K and 200 K for 10 ns each. The structure with the lowest potential energy was submitted to two consecutive MDs at 298 K for 10 ns. 100 structures were extracted from the final 10 ns with 100 ps intervals and their CCS_{th} were computed with the Trajectory Method implemented in Collidoscope.
This methodology was repeated 9 times with different Lennard-Jones parameters for H atoms. Using a fixed value of well depth (default value: 0.0152 kcal mol^{-1}), we varied the equilibrium distance between 2.75 and 3.195 Å, with the latter corresponding to the default DREIDING value. The lowest difference between the experimental and theoretical cross sections was obtained for an equilibrium distance of 2.83 Å.

In order to parametrize the well depth for hydrogen atoms, experimental and theoretical values of vaporization enthalpies were compared. Experimental values were obtained from the NIST database. Solvent boxes (propane, butane, pentane, hexane, cyclohexane and methyl acetate) were built and their vaporization enthalpies were computed using:

$$\Delta H_{vap} = \langle E_{intra} \rangle - \langle E_{total} \rangle + RT$$

where E_{total} is the total energy of the box and E_{intra} is the total energy of a single solvent molecule.
Periodic boxes containing ~ 1000 solvent atoms were generated. Initial cell parameters were adjusted to reproduce the experimental densities. Simulations were carried out using the DREIDING force field with an equilibrium distance for hydrogen atoms set to 2.83 Å (as determined above) and a well depth varied between 0.01 and 0.044 kcal mol^{-1}.
The boxes were first subjected to high-temperature MD (NVT, 750K, 50ps) and then to a room temperature MD (NVT, 298K, 100ps). A third MD was performed at high pressure (NPT, 298K, 3 GPa, 298K) for 10 ns. Finally, a last MD run was carried out at an ambient pressure until energy convergence. The computation of vaporization enthalpies was realized with Materials Studio's Forcite module. The lowest difference between NIST data and computed enthalpies was found with a well depth set to 0.0152 kcal mol^{-1} (corresponding exactly to the DREIDING default value).

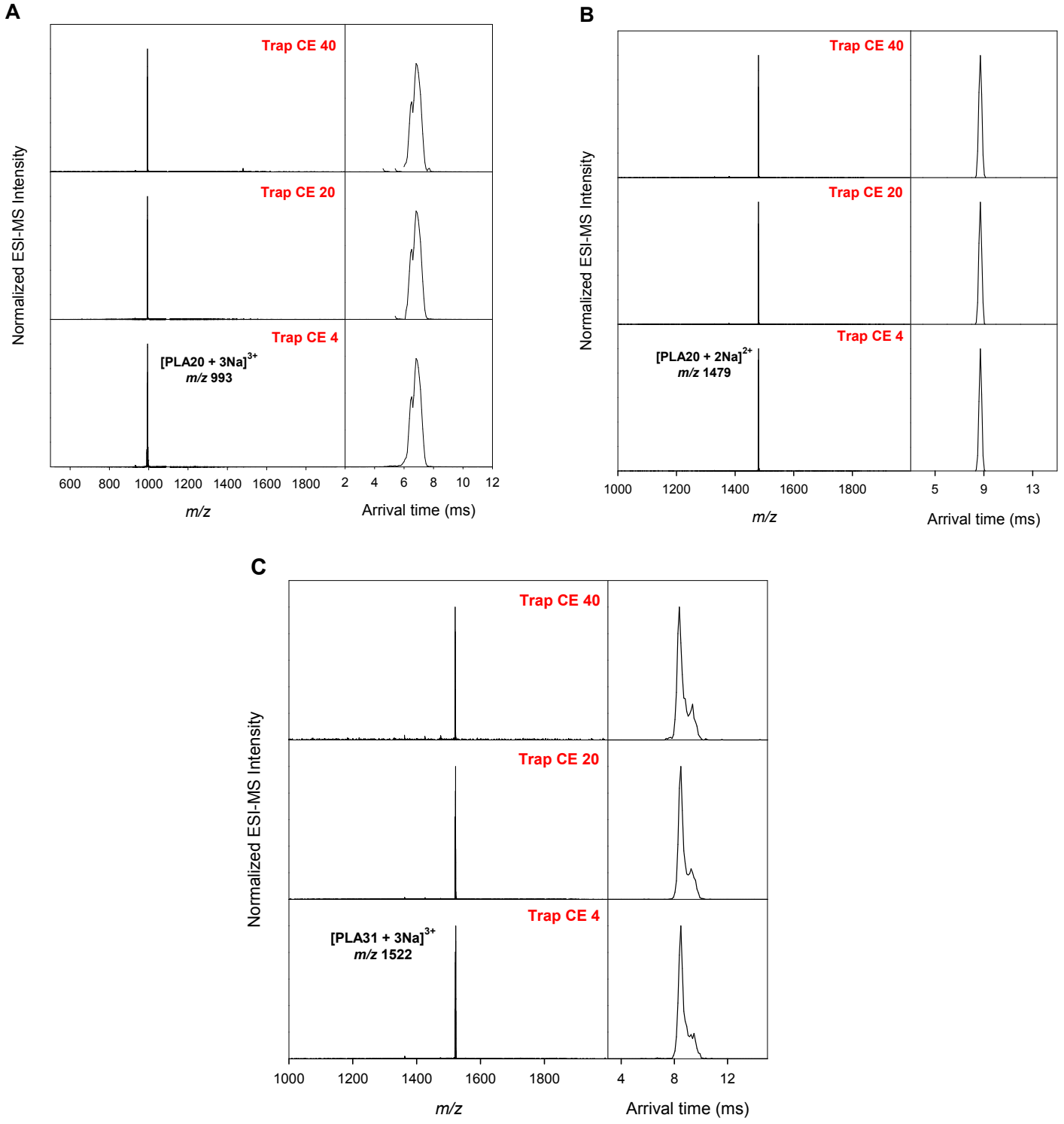

Figure S2. Mass spectra and IMS ATDs of quadrupole selected ion species recorded for (A) $[PLA20 + 3Na]^{3+}$, (B) $[PLA20 + 2Na]^{2+}$, (C) $[PLA31 + 3Na]^{3+}$) with increasing trap collision voltage (trap CE). In all cases the trap CE was low enough to avoid the rupture of covalent bonds, evident from the lack of fragment ions in the mass spectra. Consistent with tandem-IMS data previously acquired on another instrument (Ref 43 of the main text), the ATDs remain virtually unchanged during collisional activation, highlighting the kinetic stability, and the absence of structural interconversion for the coexisting gas phase conformers observed here.

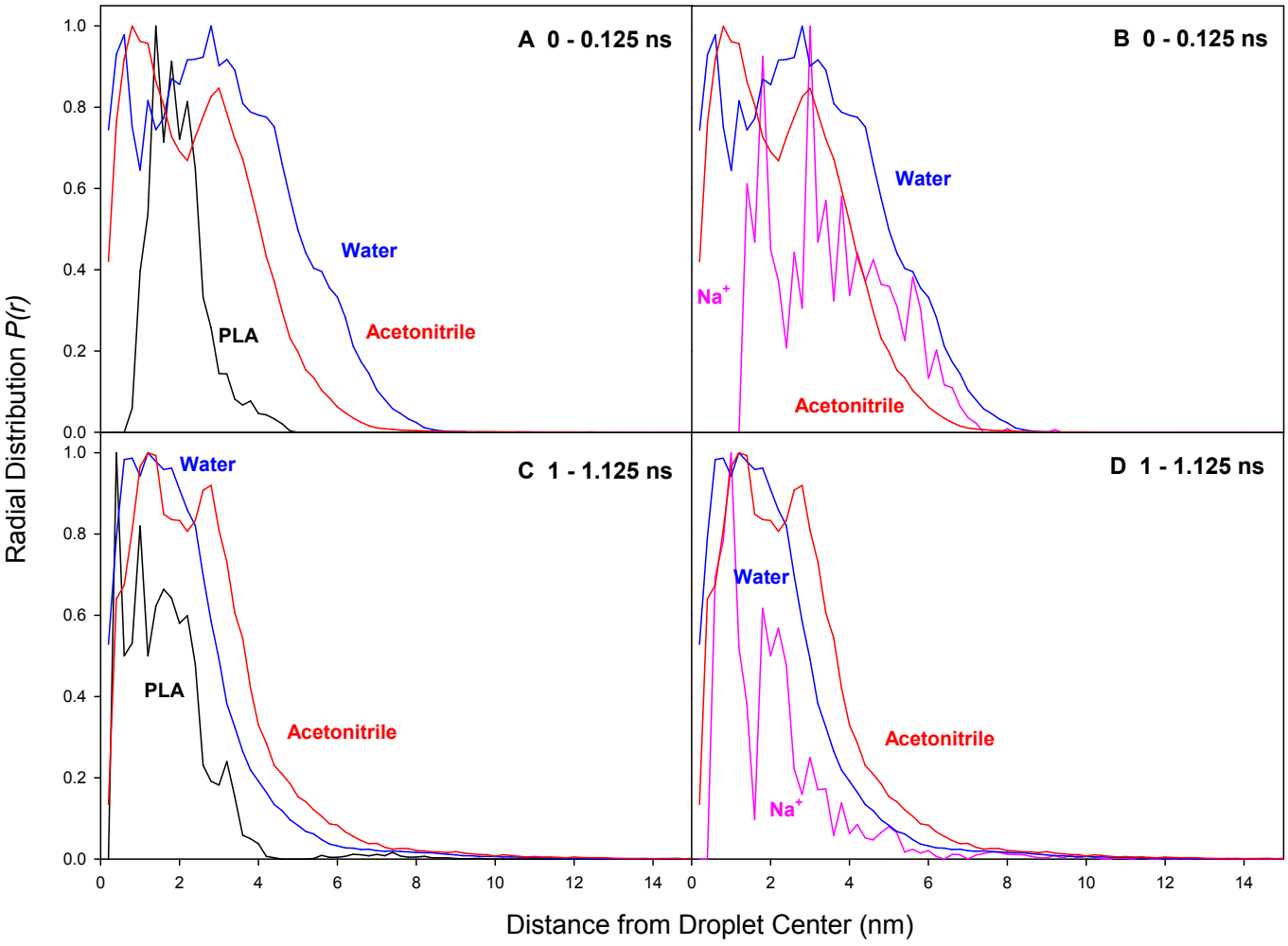

Figure S3. MD results for water/acetonitrile droplets containing PLA20, with r_0 = 5.5 nm. The four panels show normalized radial distributions of water (blue), acetonitrile (red), PLA20 (black) and Na^+ (pink), averaged for non-equilibrated droplets (t = 0 to 0.125 ns, panels A/B), and after 1 ns of equilibration (t = 1 to 1.125 ns, panels C/D).

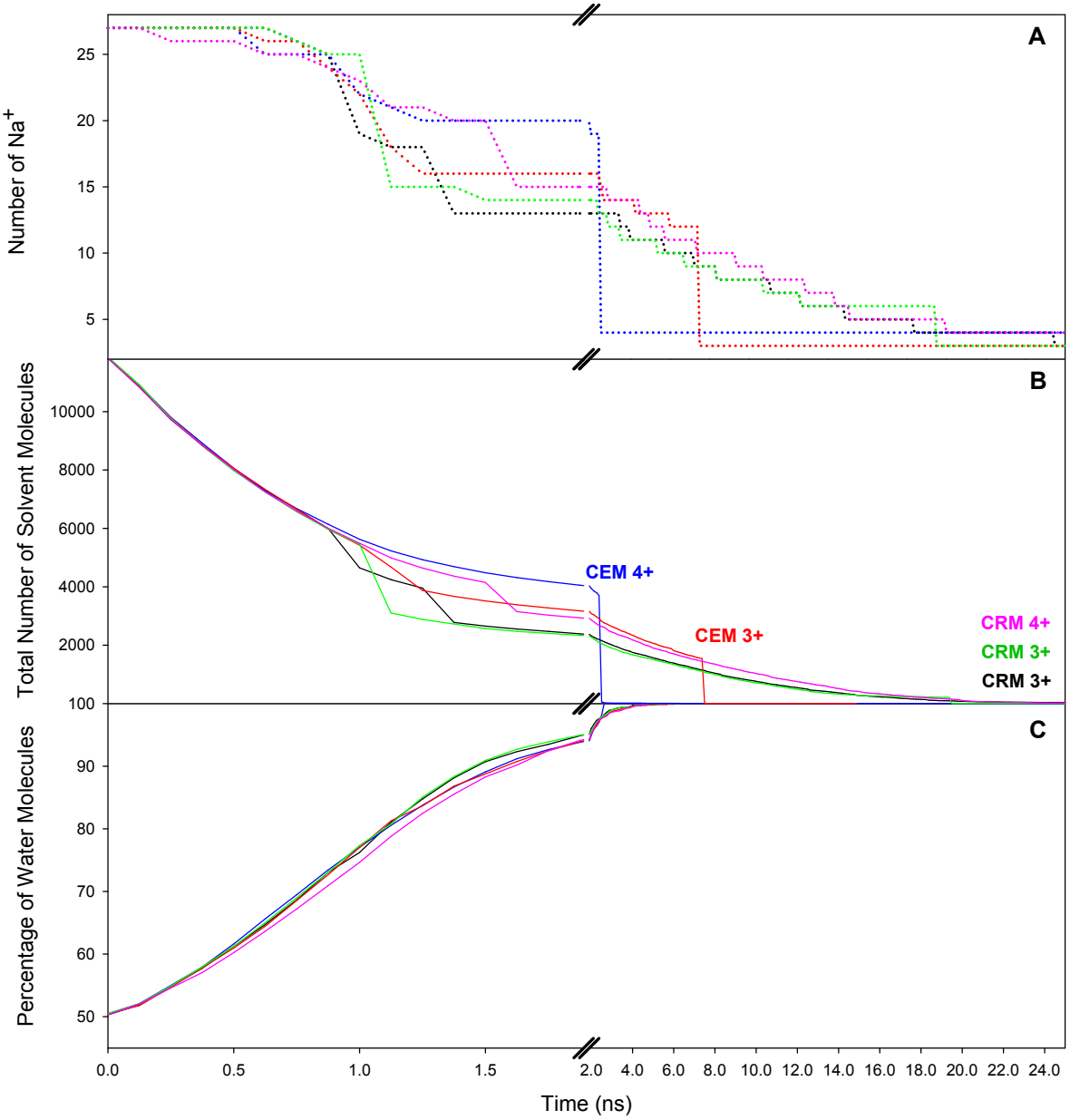

Figure S4. MD data for PLA20 in water/acetonitrile droplets (r_0 = 5.5 nm). Each color represents one simulation run, displaying (A) the number of Na^+, (B) the number of solvent molecules, and (C) the water percentage. Also indicated in panel (B) are the time points where the release of PLA20 from the droplet has gone to completion, along with the resulting charge state and the mechanism of ion formation (CRM or CEM).

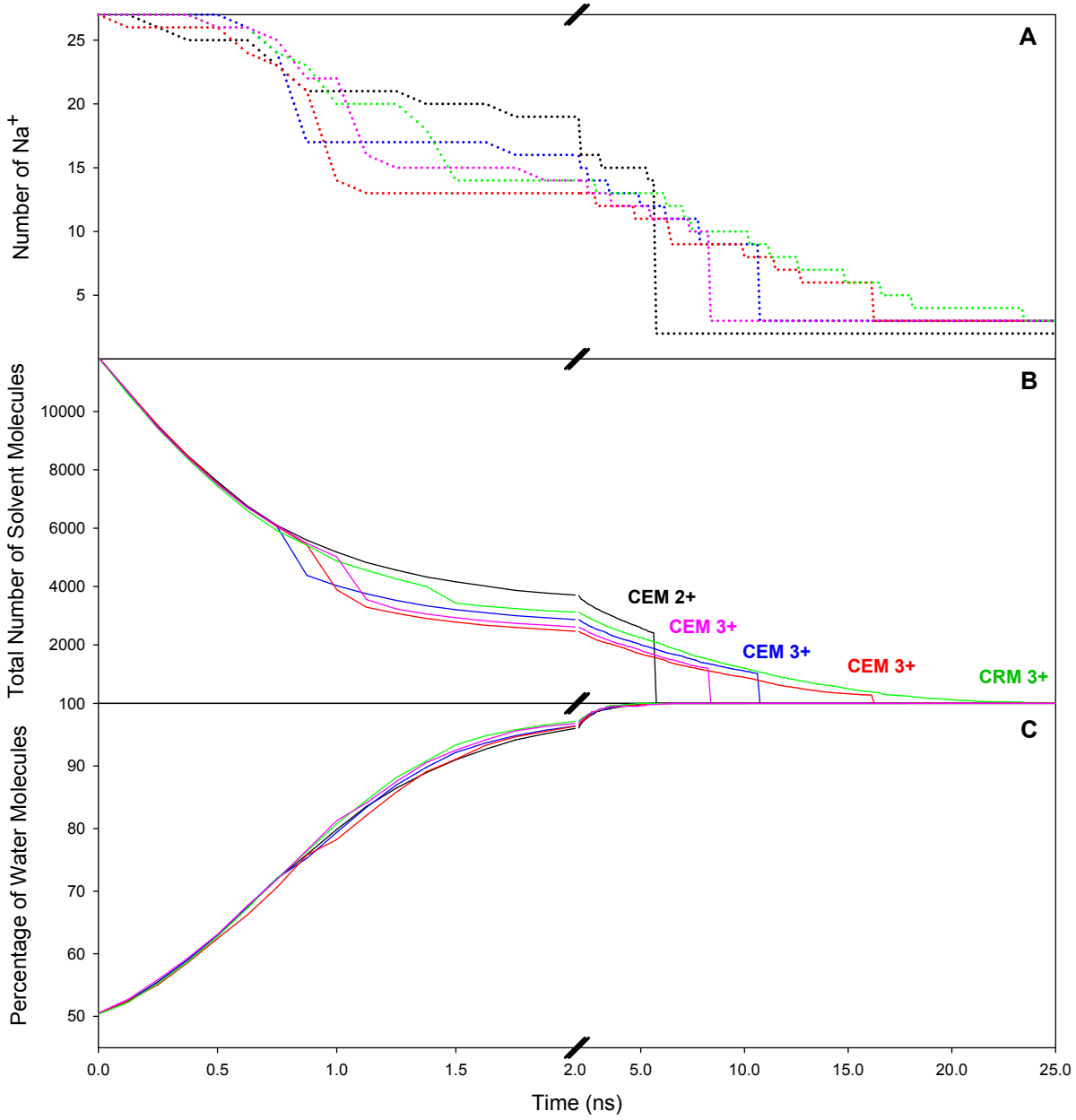

Figure S5. MD data for PLA16 in water/acetonitrile droplets (r_0 = 5.5 nm). Each color represents one simulation run, displaying (A) the number of Na^+, (B) the number of solvent molecules, and (C) the water percentage. Also indicated in panel (B) are the time points where the release of PLA20 from the droplet has gone to completion, along with the resulting charge state and the mechanism of ion formation (CRM or CEM).

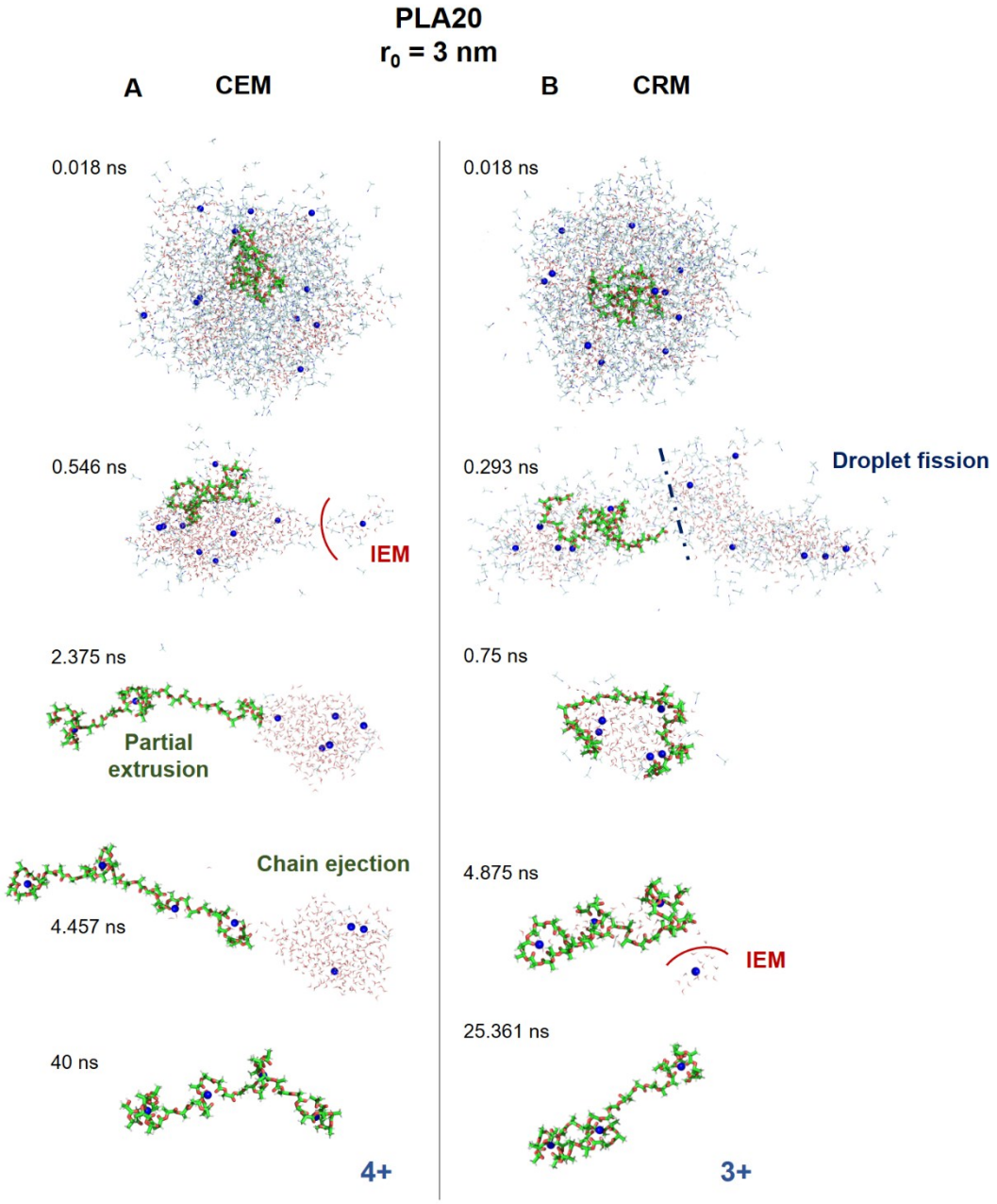

Figure S6. MD snapshots representing the ESI process obtained in two MD runs for water/acetonitrile droplets with r_0 = 3 nm containing PLA20. These data illustrate the formation of gaseous PLA20 via either (A) CEM or (B) CRM. IEM ejection of Na^+ and droplet fission events are highlighted. The final charge states of the PLA ions are indicated. PLA carbon atoms are shown in green, oxygens in red, hydrogens in white and Na^+ are shown in blue. Acetonitrile is shown in pale cyan.

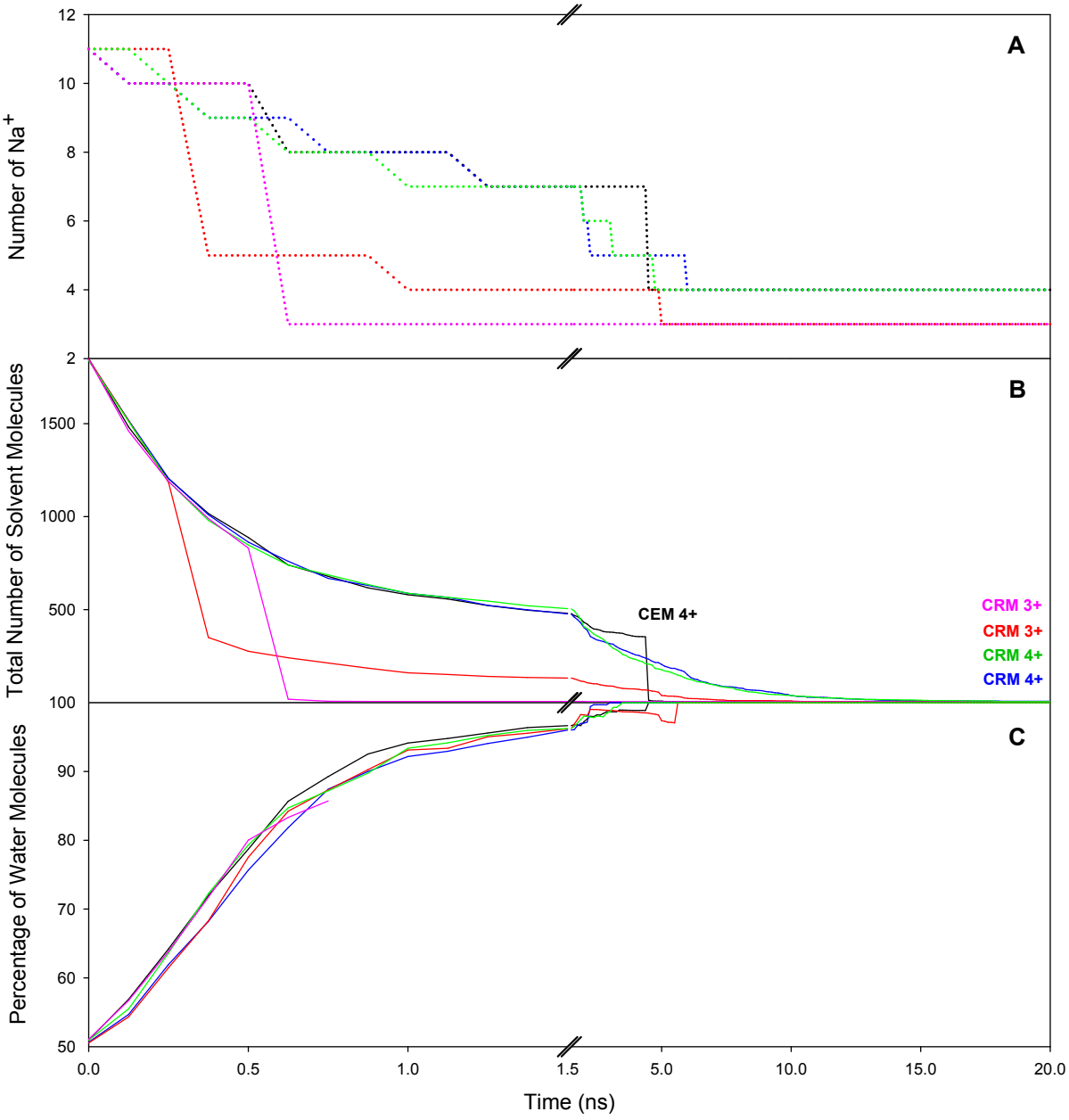

Figure S7. MD data for PLA20 in water/acetonitrile droplets (r_0 = 3 nm). Each color represents one simulation run, displaying (A) the number of Na^+, (B) the number of solvent molecules, and (C) the water percentage. Also indicated in panel (B) are the time points where the release of PLA20 from the droplet has gone to completion, along with the resulting charge state and the mechanism of ion formation (CRM or CEM).

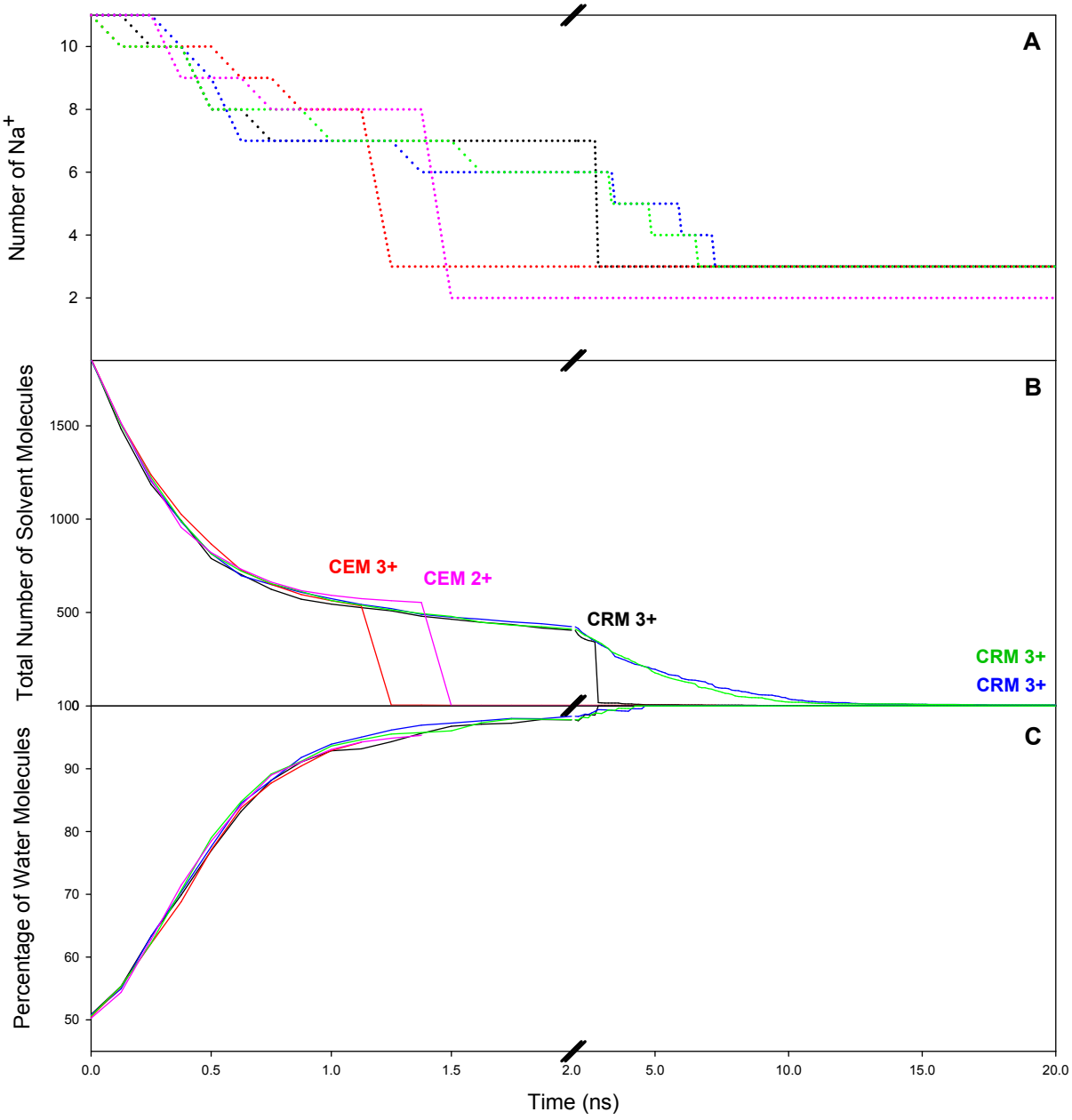

Figure S8. MD data for PLA16 in water/acetonitrile droplets (r_0 = 3 nm). Each color represents one simulation run, displaying (A) the number of Na^+, (B) the number of solvent molecules, and (C) the water percentage. Also indicated in panel (B) are the time points where the release of PLA20 from the droplet has gone to completion, along with the resulting charge state and the mechanism of ion formation (CRM or CEM).

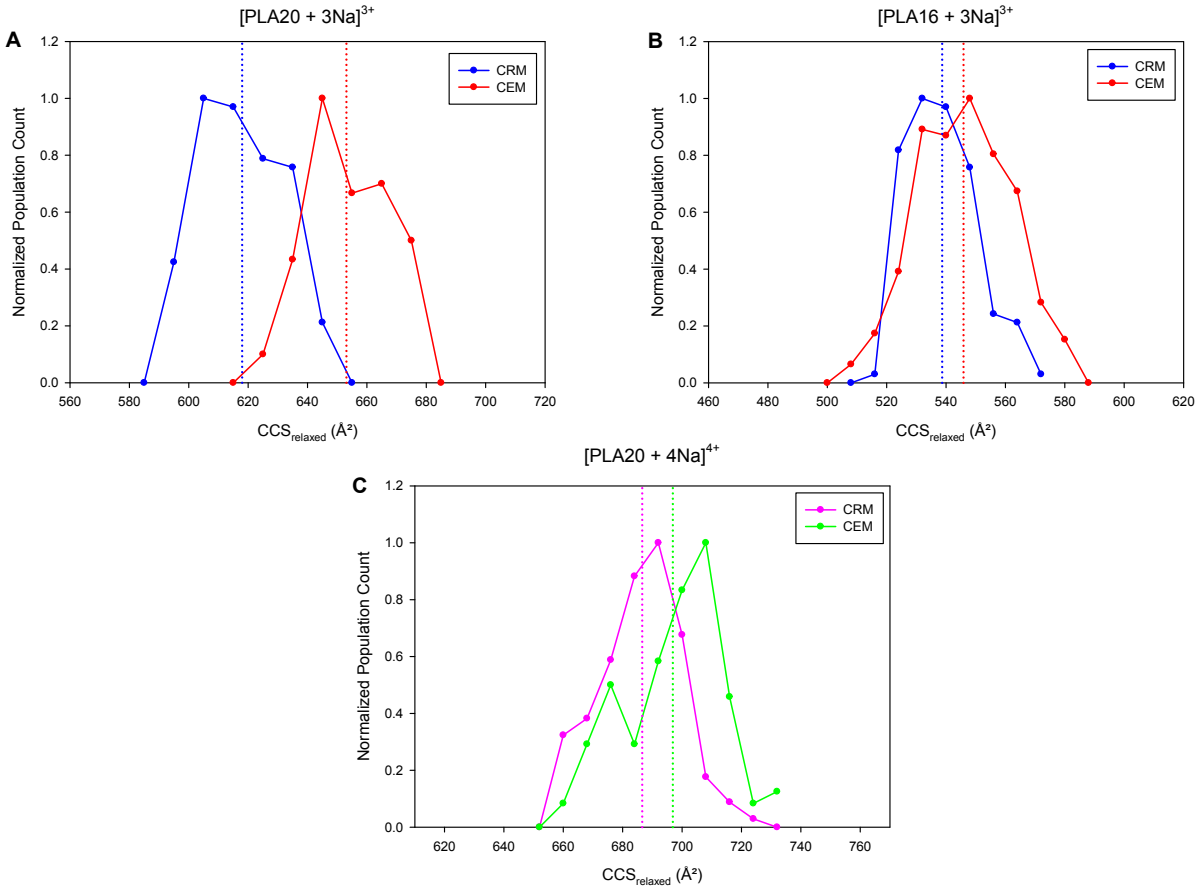

Figure S9. Histograms of simulated $CCS_{relaxed}$ values for CEM and CRM-generated ions. (A) $[PLA20+ 3Na]^{3+}$, (B) $[PLA16 + 3Na]^{3+}$, and (C) $[PLA20 + 4Na]^{4+}$. Vertical dotted lines indicate average $CCS_{relaxed}$ values for each of the distributions. $[PLA20+ 3Na]^{3+}$ shows by far the largest difference between CEM and CRM-generated ions (panel A). Statistical analyses for the data shown here are summarized in Table S1.

Ion	av. $CCS_{relaxed}$ **(CRM)**	av. $CCS_{relaxed}$ **(CEM)**	av. $CCS_{relaxed}$ difference	*t*-value	Degrees of freedom	*p*-value
$[PLA20 + 3Na]^{3+}$	618.0	653.1	5.7 %	19.09	246	< 2.2e-16
$[PLA16 + 3Na]^{3+}$	538.7	545.9	1.3 %	4.70	405	3.6e-6
$[PLA20 + 4Na]^{4+}$	686.5	696.9	1.5 %	5.24	252	3.3e-7

Table S1. Average $CCS_{relaxed}$ values of CEM and CRM-generated ions. Also included are statistical analysis results. Two-tailed t-tests yielded *p*-values < 0.001 for each of the CEM/CRM data sets, implying that relaxed CEM and CRM-generated ions adopt statistically different structures. By far the largest difference is observed for $[PLA20 + 3Na]^{3+}$.